

The Centurion 18 telescope of the Wise Observatory

Noah Brosch • David Polishook • Avi Shporer • Shai Kaspi •
 Assaf Berwald • Ilan Manulis

© Springer-Verlag ••••

Abstract We describe the second telescope of the Wise Observatory, a 0.46-m Centurion 18 (C18) installed in 2005, which enhances significantly the observing possibilities. The telescope operates from a small dome and is equipped with a large-format CCD camera. In the last two years this telescope was intensively used in a variety of monitoring projects.

Noah Brosch

The Wise Observatory and the Raymond and Beverly Sackler School of Physics and Astronomy, The Raymond and Beverly Sackler Faculty of Exact Sciences, Tel Aviv University, Tel Aviv 69978, Israel. Email: noah@wise.tau.ac.il
 David Polishook

The Wise Observatory and Department of Geophysics and Planetary Sciences, The Raymond and Beverly Sackler Faculty of Exact Sciences, Tel Aviv University, Tel Aviv 69978, Israel. Email: david@wise.tau.ac.il

Avi Shporer

The Wise Observatory and the Raymond and Beverly Sackler School of Physics and Astronomy, The Raymond and Beverly Sackler Faculty of Exact Sciences, Tel Aviv University, Tel Aviv 69978, Israel. Email: shporer@wise.tau.ac.il

Shai Kaspi

The Wise Observatory and the Raymond and Beverly Sackler School of Physics and Astronomy, The Raymond and Beverly Sackler Faculty of Exact Sciences, Tel Aviv University, Tel Aviv 69978, Israel. Email: shai@wise.tau.ac.il

Assaf Berwald

Astronomy manager of the NANA forum (<http://www.nana10.co.il>). Email: assafberwald@gmail.com

Ilan Manulis

Technoda Center for Education in Science and Technology, P.O. Box 1144 Givat Olga, Hadera 38110, Israel. Email: ilan@trendline.co.il

The operation of the C18 is now automatic, requiring only start-up at the beginning of a night and close-down at dawn. The observations are mostly performed remotely from the Tel Aviv campus or even from the observer's home. The entire facility was erected for a component cost of about 70k\$ and a labor investment of a total of one man-year.

We describe three types of projects undertaken with this new facility: the measurement of asteroid light variability with the purpose of determining physical parameters and binarity, the following-up of transiting extrasolar planets, and the study of AGN variability. The successful implementation of the C18 demonstrates the viability of small telescopes in an age of huge light-collectors, provided the operation of such facilities is very efficient.

Keywords Telescopes

1 Introduction

The Wise Observatory (WO, see <http://wise-obs.tau.ac.il>) began operating in 1971 as a Tel-Aviv University (TAU) research laboratory in observational optical astronomy. It is located on a high plateau in the central part of the Negev desert (longitude 34°45' 48" E, latitude 30°35'45" N, altitude 875 m, time zone is -2 hours relative to Universal Time). The site is about 5 km west of the town of Mitzpe Ramon, 200 km south of Tel-Aviv and 86 km south of Beer Sheva. An image of the Wise Observatory is shown in Figure 1.

The WO was originally equipped with a 40-inch telescope (T40). The Boller and Chivens telescope is a wide-field Ritchey-Chrétien reflector mounted on a rigid, off-axis equatorial mount. The optics are a Mount Wilson/Palomar Observatories design, consisting of a 40-inch diameter clear aperture f/4 primary mirror, a 20.1-inch diameter f/7 Ritchey-Chrétien secondary mirror, and a quartz corrector



Fig. 1.— The Wise Observatory observing facilities. From left to right: the dome of the T40 and main building, the dome of the C18, and the box enclosure of the WHAT.

lens located 4 inches below the surface of the primary mirror, providing a flat focal field of up to 2.5 degrees in diameter with a plate scale of $30 \text{ arcsec mm}^{-1}$. An $f/13.5$ Cassegrain secondary mirror is also available, but is hardly used nowadays. This telescope was originally a twin of the Las Campanas 1m Swope telescope, described by Bowen & Vaughan (1973), though the two instruments diverged somewhat during the years due to modifications and upgrades. The telescope is controlled by a control system located in the telescope room.

In its 36 years of existence the observatory has kept abreast of developments in the fields of detectors, data acquisition, and data analysis. In many instances the observations can now be performed remotely from Tel Aviv, freeing the observer from the necessity to travel to the observing site. The efficiency of modern detectors implies that almost every photon collected by the telescope can be used for scientific analysis.

The on-going modernization process allowed landmark studies to be performed and generations of students to be educated in the intricacies of astronomy and astrophysics. Some of these students are now staff members of the Physics and Astronomy Department at TAU or at other academic institutions in Israel or overseas. The one-meter telescope is over-subscribed, with applications for observing time exceeding by $\sim 50\%$ the number of available nights. This demonstrates the vitality of the observatory as a research and academic education facility, even though on a world scale the size of the telescope shrank from being a medium-sized one in the early-1970s to being a “small” telescope nowadays.

The Wise Observatory operates from a unique location, in a time zone between India and Greece and in a latitude range from the Caucasus to South Africa, where no other modern observatories exist, and at a desert site with a large fraction of clear nights. Thus, even though its 1m telescope

is considered small, it is continuously producing invaluable data for the study of time-variable phenomena, from meteors and extrasolar planet searches to monitoring GRBs and microlensing events, to finding distant supernovae and “weighing” black holes in AGNs. A cursory literature search shows that the Wise Observatory has one of the greatest scientific impacts among 1m-class telescopes.

One research aspect that developed into a major WO activity branch is of time-series studies of astronomical phenomena. A project to monitor photometrically and spectroscopically Active Galactic Nuclei (AGNs) is still running, following about 30 years of data collection. Other major projects include searches for supernovae or for extrasolar planets (using transits or lensing events), observations of novae and cataclysmic variables, studies of star-forming galaxies in a variety of environments, and studies of Near Earth Objects (NEOs) and other asteroids. These studies, mainly part of PhD projects, are observation-intensive and require guaranteed telescope access for a large number of nights and for a number of years. The oversubscription of the available nights on the T40, the need to follow-up possible discoveries by small telescopes with long observing runs, and a desire to provide a fallback capability in case of major technical problems with the T40, required therefore the expansion of the WO observational capabilities.

Small automatic, or even robotic, instruments provide nowadays significant observing capability in many astronomy areas. Combining these small telescopes into a larger network can increase their scientific impact many-fold. This is currently done with the GCN (Barthelmy *et al.* 1998). Examples of such instruments are REM (Zerbi *et al.* 2001), WASP and super-WASP (e.g., Pollacco *et al.* 2006), HAT (Bakos *et al.* 2004), and ROTSE-III (e.g., Akerlof *et al.* 2003; Yost 2006), and very recently KELT (Pepper *et al.* 2007). Among the larger automatic instruments we mention the Liverpool Telescope (e.g., Steele *et al.* 2004) and its

clones. Such automatic instruments enable the exploration of the last poorly studied field of astronomy: the temporal domain. However, a first step before developing a network of automatic telescopes is demonstrating feasibility at a reasonable cost for a single, first instrument. This paper describes such an experiment at the Wise Observatory in Israel.

2 The telescope

To enhance the existing facilities with special emphasis on time-series astronomy, we decided in 2002 to base an additional observing facility on as many off-the-shelf hardware and software components as possible, to speed the development and bring the new facility on-line as soon as possible. We decided to acquire a Centurion 18 (C18) telescope manufactured by AstroWorks, USA. The telescope was delivered towards the end of 2003 and operated for a year in a temporary enclosure. From 2005 the telescope operates in its permanent dome, which is described below. The C18 has a prime-focus design with an 18-inch (0.46-m) hyperbolic primary mirror figured to provide an $f/2.8$ focus. The light-weighted mirror reflects the incoming light to the focal plane through a doublet corrector lens. The telescope is designed to image on detectors as wide as regular (35-mm) camera film though with significant edge-of-field vignetting, but we now use a much smaller detector, and the images are very reasonable indeed ($\text{FWHM} \sim 2''.9$ at the edge of the CCD, only 13% worse than at field center, with most image size attributable to local seeing).

The focal plane is maintained at the proper distance from the primary mirror by a carbon-reinforced epoxy plastic (CREP) truss tube structure. The support tubes allow the routing of various wires and tubes (see below) through the structure, providing a neat construction and much less vignetting than otherwise. The CREP structure has a very low expansion coefficient; this implies that the distance between the primary and the focal plane hardly changes with temperature. The stiff structure and the relatively low loading of the focal plane imply that the telescope hardly flexes with elevation angle.

The optical assembly uses a fork mount, with the right ascension (RA) and declination (DEC) aluminum disk drives being of pressure-roller types. The steel rollers are rotated by stepping motors and both axes are equipped with optical sensors, thus the motions of the telescope can be controlled by computer. The fork mount and the truss structure limit the telescope pointing to north of declination -33° .

The focal plane assembly permits fine focusing using a computer-controlled focuser connected to the doublet corrector and equipped with a stepper motor. The C18 was originally supplied with a primary mirror metal cover that had to be removed manually. Since then, an electrically-operated, remotely-commanded mirror cover was installed.

3 The CCD

The telescope was equipped from the outset with a Santa Barbara Instrument Group (SBIG) ST-10 XME USB CCD camera that was custom-fitted to our specific telescope by AstroWorks and was delivered together with the telescope. This thermoelectrically-cooled chip has 2184×1472 pixels each $6.8 \mu\text{m}$ wide, which convert to 1.1 arcsec at the $f/2.8$ focus of the telescope. The chip offers, therefore, a $40'.5 \times 27'.3$ field of view. A second, smaller CCD, mounted next to the science CCD, allows guiding on a nearby star using exactly the same optical assembly. The CCD is used in “white light” with no filter. The readout noise is 10 electrons per pixel and the gain is 1.37 electrons per count. Each FITS image is 6.4 MB and the read out time is ~ 15 sec using the *MaximDL* package.

The CCD is mounted behind the doublet corrector lens and the focusing is achieved by moving the lens. In practice, even though the beam from the telescope is strongly converging, the focus is fairly stable throughout the night despite ambient temperature excursions of $\sim 10^\circ\text{C}$ or more. In any case, refocusing is very easy using the automatic focuser.

After a few months of test operations, we decided to add water cooling to the ST-10. This was achieved by feeding the inlet water port of the SBIG CCD with an antifreeze solution from a one-liter reservoir that was continuously circulated by an aquarium pump. The addition of water cooling reduced the CCD temperature by an additional 10°C , lowering the dark counts to below 0.5 electrons $\text{pixel}^{-1} \text{sec}^{-1}$. We emphasize that the water circulation operates continuously, 24 hours per day, irrespective of whether the telescope is used for observations or not. Since its implementation, we changed the cooling fluid only once when it seemed to develop some kind of plaque.

The CCD is used in “white light” without filters to allow the highest possible sensitivity. The chip response reaches 87% quantum efficiency near 630 nm, implying an overall response similar to a “wide-R” band.

The effective area of the telescope and CCD is shown in Figure 3. This was calculated using the generic CCD response from the SBIG web site for the Kodak enhanced KAF-3200ME chip, assuming 7% areal obscuration of the primary mirror by the secondary mirror baffle and CCD, 80% mirror reflectivity, and 5% attenuation at each surface by the doublet lens and CCD window.

4 The dome

Given the small size of the telescope and the high degree of automation desired, we chose a small dome that would not allow routine operation with a human inside, but would allow unrestricted access to the sky for the C18. From among



Fig. 2.— The Centurion 18 telescope viewed through the dome slit, with the dome door opened. Note the anti-collision switches mounted at the top of the truss structure and on the equatorial fork, and the electrically-operated primary mirror cover, here in the open position.

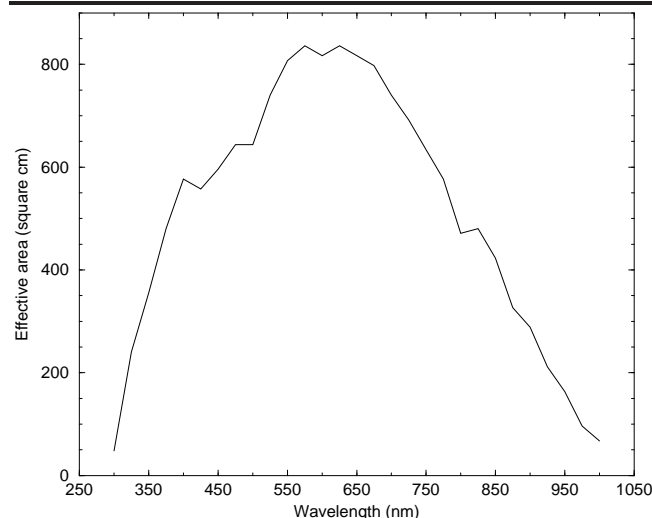


Fig. 3.— Effective area of the C18 telescope with the SBIG ST-10XME CCD.

the off-the-shelf domes we chose a Prodome 10-foot dome from Technical Innovations USA¹, equipped with two wall rings to provide sufficient height for the C18 in all directions.

The fiberglass dome was equipped by Technical Innovations with an electrical shutter and with the necessary sensors to operate the *Digital Dome Works (DDW)* software bundled with the dome; this allows control of all the dome functions from a computer equipped with a four-port Multi-I/O card, adding four serial ports to the two already available on the operating computer. In addition, we equipped the dome with a weather station mounted on a nearby mast, a video camera with a commandable light source that allows remote viewing of the telescope and of part of the dome to derive indications about its position, and a “Robo reboot” device for *DDW*. The latter was installed to allow the remote initialization of the dome functions in case of a power failure.

Later, we added a Boltwood Cloud Sensor² that measures the amount of cloud cover by comparing the temperature of the sky to that of the ambient ground. The sky and ground temperatures are determined by measuring the amount of radiation in the 8 to 14 micron infrared band. A large difference indicates clear skies, whereas a small difference indicates dense, low-level clouds. This allows the sensor to continuously monitor the clarity of the skies, and to trigger appropriate alerts on the control computer. The device also includes a moisture sensor that directly detects rain drops.

The dome and the operating computer are connected to the mains power supply through a “smart” UPS that will shut down the observatory in case of an extended power outage.

The dome and telescope are mounted on a circular reinforced concrete slab with a 3.5-m diameter and 0.5-m thickness. The concrete was poured directly on the bedrock, which forms the surface ground layer at the WO site. The dome and the concrete slab are shown in Figure 4.

5 The operating software

We decided that all the software would be tailored into a suite of operating programs that would conform to the *ASCOM* standards³. This is in contrast with other similar, but significantly more expensive, small automatic observatories (e.g., Akerloff *et al.* 2003), which chose various flavors of LINUX. Our choice saved the cost in money and time of developing specialized software by using off-the-shelf products. It also facilitated a standard interface to a range of astronomy equipment including the dome, the C18 mount, the focuser and the camera, all operating in a Microsoft Windows environment.

The *ACP* (Astronomer’s Control Program) software is a product of DC-3 Dreams⁴. *ACP* controls the telescope motion and pointing, and can change automatically between different sky fields according to a nightly observing plan. *ACP* also solves astrometrically the images collected by the CCD, and improves automatically the pointing of the telescopes using these solutions. The program communicates with and controls the operating software of the dome, interfacing with *DDW*, enabling one to open and close the dome shutter, and commanding the dome to follow the telescope

¹<http://www.homedome.com/>

²http://www.cyanogen.com/products/cloud_main.htm

³Astronomy Common Object Model, <http://ascom-standards.org/>

⁴<http://acp.dc3.com/>



Fig. 4.— The C18 dome, with DP looking through the dome shutter to the telescope.

or to go to a “home” position. In addition, the *ACP* software is a gateway to the *MaximDL*⁵ program that operates the CCD. Different types of exposures, guiding and cooling of the CCD can be commanded manually using *MaximDL*, but in most cases we use the *ACP* code envelope (the *AcquireImages* script) to operate the entire system. The focusing is also done automatically using the freeware *FocusMax*⁶, a software package that operates the Robo-focus and searches automatically for the best FWHM of a selected star.

To enable power shut-down by remote users we connected the telescope, dome, CCD, focuser and the telescope’s cover to a relay box that is connected to the six serial ports on the computer. Using a self-written code (*C18 control*) the remote user can enable or disable the electrical power supply to the different components of the system and open or close the telescope cover. This guarantees the safety of the equipment during daytime and enables the astronomer to fully operate the system from a remote location using any VNC viewer software. Figure 5 exhibits the different programs making up the software environment, their connections and their hierarchy.

6 Cost

The affordability of an automatic telescope is an important consideration for many observatories. We found that it was not possible to collect sufficient funds to cover the high cost of an off-the-shelf automatic telescope with similar capabilities to those of the installation described here.

The C18 telescope, CCD, and dome, including all the electronic add-ons and the software, added up to slightly more than 70k\$. To this one should add significant in-house contributions; the dome was received in segments that were erected and bolted on the concrete slab by WO staff Ezra Mash’al and Sammy Ben-Guigui together with NB; the installation, tuning-up and interfacing of the various software components were done mainly by IM, DP, and AB; the polar alignment of the C18 was done (twice) by AB who also developed the electrically-operated primary mirror cover. All these and more would add up to about a person-year of work by very experienced personnel.

7 Performance

The automated operation mode of the C18 makes it an easy telescope to use, demanding from the astronomer only to watch the weather conditions when these are likely to

change. Overall, the C18’s performance and output are satisfying.

The telescope slewing time is about 5° sec^{-1} on both axes and the settling-down time is 5-8 sec. The dome rotates at a rate of 3.33 degrees per second in each direction, while its response time in following the telescope motion is 2-3 sec. Opening the dome shutter requires 55 sec and closing it 70 sec, with the dome parked at its “home” location. Opening or closing the electrical telescope cover requires 20 sec.

The auto-guiding system, which uses a smaller CCD in the same camera head, maintains round stellar images even for the longest exposures that are limited by the sky background, although the telescope is not perfectly aligned to the North. Without the guider, one can expect round star images only for exposure times of 90 sec or shorter. In some cases, telescope shake is experienced due to wind blows. Since the wind at the WO usually blows from the North-West, and usually slows down a few hours into the night, selecting targets away from this direction for the first half of the night decreases the number of smeared images to a minimum.

The pointing errors of the C18 are of order 10 seconds of time in RA and 30 to 60 arcsec in DEC. However, astrometrically solving the images using the *PinPoint*⁷ engine, which can be operated automatically by the *ACP* software immediately following the image readout, re-points the telescope to a more accurate position for the following images of the same field.

Since the CCD cooling is thermoelectric with water-assistance, with the cooling water at ambient temperature, the CCD temperature depends very much on the weather. The usual values run between -15°C in the summer nights with ambient temperatures of $+30^\circ\text{C}$ to -30°C in the winter (-5°C ambient; see Figure 6). All images are acquired with the CCD cooling-power at less than 100% capacity, assuring a steady chip temperature throughout the observation.

The image read-out using *MaximDL* takes 15 sec. In regular observations an additional 10 sec interval is required for the astrometric solution of the image and another 5 sec to write the image on the local computer. A five-sec delay is required by the CCD before it continues to the next image for guider activation. Since the performance of the astrometric solution and the activation of the auto-guiding operation are user-selectable, the off-target time between sequential images is 15–30 sec, yielding a duty fraction of 83–92% on-sky time for typical 180 sec exposures.

The CCD bias values are 990 ± 5 counts, a value which is cooling-dependent. The bias values changed from an original ~ 110 to the present value after one year of use and a rebuild of the software following a disk crash. The CCD flat field (FF) shows a 1.2% standard deviation from the image median. The FF gradient is steeper at the southern corners of the images than at the northern corners, as seen in

⁵http://www.cyanogen.com/products/maxim_main.htm

⁶<http://users.bsdwebsolutions.com/larryweber/>

⁷<http://pinpoint.dc3.com/>

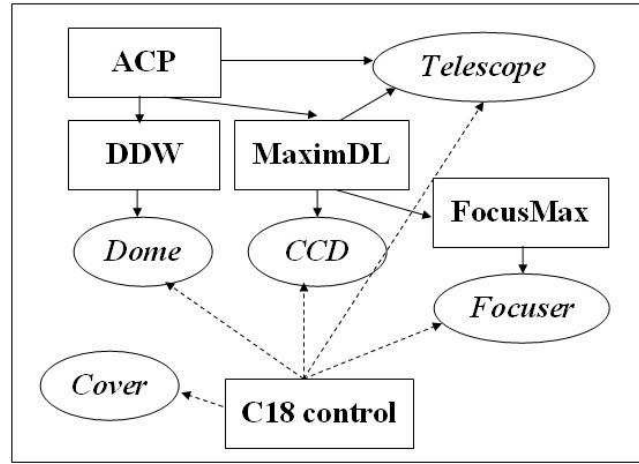


Fig. 5.— The C18 software hierarchy. Different programs are represented by rectangles and hardware items by ellipses. Dashed links represent electrical power on/off connections.

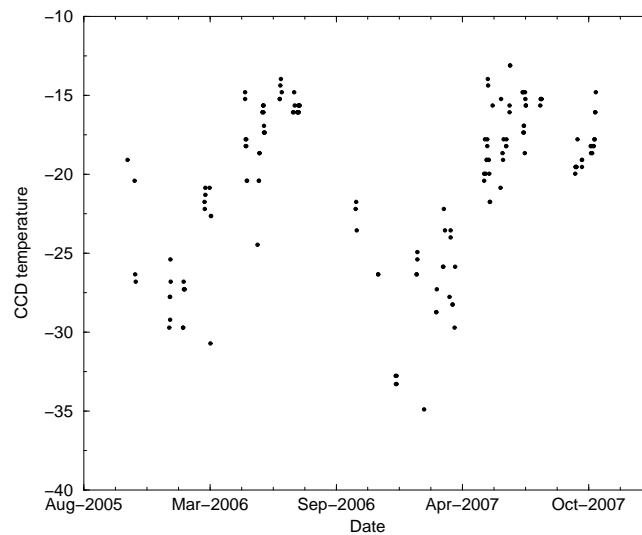


Fig. 6.— CCD night-time temperature during two years starting on 25 October 2005, as read from the automatically-generated FITS header of the images. The chip is warmer in the summer because the hot end of the thermoelectric cooler is in contact with water at ambient temperature, and this is warmer in the summer.

Figure 7. This probably reflects some additional vignetting in the telescope on top of the prime focus baffle, possibly caused by the asymmetric blockage by the SBIG CCD, and by the pick-off prism edge for the TC-237H tracking CCD, mounted next to the science CCD, which is used for guiding. Twilight flats give the best results, provided the CCD cooling is started at least 30 min before obtaining the flat field images.

On a dark night with photometric conditions the sky background is 10–15 counts per pixel per second. Comparing with the R-band magnitude of standard stars (Landolt 1992) the sky as measured on the C18 images in the “wide-R” band is about 20.4 mag arcsec⁻¹ and stars of 19.5 magnitudes are detectable with $S/N \simeq 25$. This fits well previous measurements of the sky brightness at the Wise Observatory ($\mu_R \simeq 21.2$ mag arcsec⁻¹ in 1989; Brosch 1992), accounting for the slight site deterioration in the last 15 years due to ambient light sources and for the wider spectral bandpass.

8 Lessons learned

8.1 Dome electrical contacts

The dome shutter opening mechanism receives its 12V DC electrical supply from two spring contacts that touch metal pads on the dome inner circumference. These spring contacts are made of slightly elastic copper strips twisted into rings and are fixed to the dome. To maintain electrical contact, the copper strips brush against a scouring pad before reaching the fixed contacts on the dome rim to scrape off accumulated dirt and oxide.

During the two years of operating the C18 we have had the strips break a number of times. This interrupts the electrical contacts to the dome shutter and may prove dangerous when bad weather arrives in case nobody is present at the WO, since it prevents the remote shutting of the dome. The remedy is replacing the copper strips at regular intervals, even though they may appear intact.

8.2 Dome lift-offs

We experienced two instance of the dome lifting off its track on the stationary part of the dome enclosure. In these instances the dome slips off its track and has to be resealed manually. Since the fiberglass structure is very light, this operation can be done by a single person.

We suspect that the dome lift-off events were caused by operator error. The dome rides on a track that is segmented and passes over a short door that must be latched shut when rotating the dome. If this is not done, the door might open slightly causing the dome to derail.

8.3 Sticky dome shutter

We experienced a number of instances when the dome indicated that the shutter was closed, but inspection with the video camera showed that the shutter was still open. We have not yet tracked down the roots of this problem but it may be linked to a limitation of the electrical power to the shutter motor, perhaps connected with the operation of a low-voltage DC motor in conditions of high humidity.

Note that this type of fault requires rapid human intervention to prevent damage to the telescope and electronics in changing atmospheric conditions.

8.4 Operation in a dusty and hot desert environment

Upon ordering of the PD-10 dome we worried about the possibility of dust entering the dome while closed, specifically in case of a dust storm. These storms are rare but can deposit significant amounts of dust on optics and mechanisms in a short time. This is why we specified that the dome be equipped with thick brushes that would prevent most of the dust from entering the (closed) dome.

The two-year operational experience showed that the anti-dust brushes do indeed protect the interior of the dome and that the dust deposit on surfaces within the PD-10 dome is similar to that in the T40 dome. However, after two years of operation, the brush hairs are no longer straight but show curling and the dust prevention is no longer optimal. The brushes probably require replacing.

The daytime external temperature at the WO can reach +40°C and the inside of the dome can indeed become very hot. To prevent this, we plan to air condition the dome during daytime. This will also cool the huge concrete slab on which the telescope and dome are mounted, providing a cold reservoir for night-time operation. Daytime cooling will hopefully improve the night-time seeing by removing part of the “dome seeing” of the C18.

8.5 Anti-collision switches

In remote or automatic operation there exists a possibility that the telescope may become stuck in tracking mode, by-passing the software horizon limits. In this case, it is possible that the C18 may drive itself into the concrete floor or into the telescope fork causing instrumental damage. To prevent this, contact switches were installed on three corners at the top of the truss structure. A similar microswitch is activated by the truss structure if it approaches the base of the telescope fork (see Figure 2). These switches cut off instantly the power supply through the UPS, in case any of the switches are activated. Since such an event is primarily an operator error, we arranged that the reset of the mechanism can only be done manually, by someone physically pressing the reset button from within the dome.

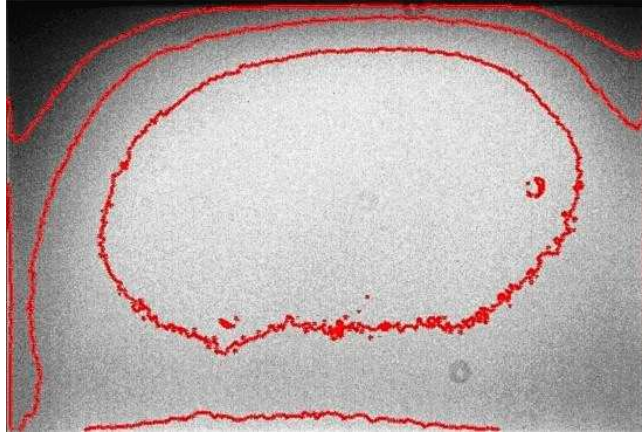


Fig. 7.— Flat field obtained with the C18 telescope and the SBIG ST-10 XME CCD. The overplotted contours are spaced by 0.0137% of the mean image value, to emphasize the flat field uniformity.

9 Scientific results

The C18 is used by different researchers at the Tel-Aviv University for various goals. Some examples, with representative outputs, are given below. We describe studies of physical parameters of asteroids, the investigation of extrasolar planets, and the monitoring of variable AGNs.

9.1 NEOs and other asteroids

Understanding the potential danger of asteroid collisions on Earth has encouraged extensive research in recent years. Knowledge of physical properties of asteroids such as size, density and structure is critical for any future mitigation plan. At WO we focus on photometry, which allows the derivation of valuable data on asteroid properties: periodicity in light curves of asteroids coincides with their spins; shape is determined by examining the light curve amplitude; axis orientation is derived by studying changes in the light curve amplitude; special features in the light curves, such as eclipses, may suggest binarity and can shed light on the object structure and density.

The C18 is mainly used for differential photometry of known asteroids as a primary target, but also enables the detection of new asteroids. The large field of the CCD allows the asteroids to cross one CCD field or less per night, even for the fast-moving Near-Earth Objects (NEOs) that can traverse at angular velocities of $0.1'' \text{ sec}^{-1}$ or slower. This ensures that the same comparison stars are used while calibrating the differential photometry. Exposure times between 30 to 180 sec are fixed for every night, depending on the object's expected magnitude and angular velocity, the nightly seeing, and the sky background. The lower limit for the signal to noise ratio of acceptable images is ~ 10 , thus asteroids that move too fast ($\geq 0.1''/\text{sec}$) or are too faint ($\geq 18.5 \text{ mag}$) are de-selected for observation. Objects brighter than

13 mag are also avoided, to prevent CCD saturation. The images are reduced using bias, dark and normalized flat field images. Time is fixed at mid-exposure for each image. The IRAF *phot* function is used for the photometric measurements. Apertures of four pixel ($\sim 4.5 \text{ arcsec}$) radius are usually chosen. The mean sky value is measured in an annulus with an inner radius of 10 pixels and a width of 10 pixels around the asteroid. The photometric values are calibrated to a differential magnitude level using 100-500 local comparison stars that are also measured on every image of a specific field. For each image a magnitude shift is calculated, compared to a good reference image. Stars whose magnitude shift is off by more than 0.02 mag from the mean shift value of the image are removed at a second calibration iteration. This primarily solves the question of transient opacity changes, and results in a photometric error of $\sim 0.01 \text{ mag}$.

Most of the observed asteroids are followed-up on different nights; this changes the background star field. Some asteroids are also observed at different phase angles and their brightness can change dramatically from one session to another. To allow comparisons and light curve folding to determine the asteroid spin, the instrumental differential photometric values are calibrated to standard R-band magnitudes using ~ 20 stars from the Landolt equatorial standards (Landolt 1992). These are observed at air masses between 1.1 to 2.5, while simultaneously observing the asteroid fields that include the same local comparison stars used for the relative calibration. Such observations are done only on photometric nights.

The extinction coefficients and the zero point are obtained using the Landolt standards after measuring them as described above. From these, the absolute magnitudes of the local comparison stars of each field are derived, followed by a calculation of the magnitude shift between the daily weighted-mean magnitudes and the catalog magnitudes of the comparison stars. This magnitude shift is added

to the photometric results of the relevant field and asteroid. The procedure introduces an additional photometric error of 0.02-0.03 mag. Since the images are obtained in white light, they are calibrated by the Landolt standards assuming the measurements are in the Cousins R system. In addition, the asteroid magnitudes are corrected for light travel time and are reduced to a Solar System absolute magnitude scale at a 1 a.u. geocentric and heliocentric distance, to yield $H(1, \alpha^0)$ values (Bowell et al. 1989).

To retrieve the light curve period and amplitude, the data analysis includes folding all the calibrated magnitudes to one rotation phase, at zero phase angle, using two basic techniques: a Fourier decomposition to determine the variability period(s) (Harris & Lupishko 1989) and the H-G system for calibrating the phase angle influence on the magnitude (Bowell et al. 1989). The best match of the model light curve to the observations is chosen by least squares. An example is shown on Figure 8 where a simple model was fitted to the observed data points of the asteroid (106836) 2000 YG₈. Figure 9 displays the folded light curve from which the rotation period P is deduced (here $P=20.2 \pm 0.2$ hours).

While the main advantage of the wide field of view of the C18 is the ability to observe even a fast-moving NEO in the same field during one night (Polishook & Brosch 2007), the instrument allows also the simultaneous monitoring of the light variations from several asteroids in the same field of view. Looking at Main Belt asteroids, many objects can be seen sharing the same field (our recent record is 11 objects in one field; see Figure 10). An exposure time of ~ 180 seconds is needed to detect this amount of asteroids while avoiding the smearing of their images due to their angular motion.

In addition to the rapid increase of our asteroid light curve database, due to this efficient observing method, new asteroids are discovered on the same images used for light curve derivation, proving that 18-inch wide-field telescopes can contribute to the detection of unknown asteroids even in the age of Pan-STARRS and other big, automated NEO-survey observatories. We emphasize that the discovery of new asteroids is **not** a goal of our research programs, but is a side-benefit. Our records indicate that by observing in the direction of the main belt we can detect a new asteroid in every 2-3 fields. These objects are reported to the MPC, but are not routinely followed up.

The ACP software can move the telescope automatically between different fields, increasing the number of measured asteroids. With the telescope switching back and forth between two fields, the photometric cost is the increase of the statistical error by $\sqrt{2}$, since the exposure time is reduced by half for each field, but the number of measured light curves obtained every night is very high.

9.2 Extrasolar planets

A *transiting* extrasolar planet crosses the parent star's line-of-sight once every orbital revolution. During this crossing,

referred to as a transit, which usually lasts a few hours, the planet blocks part of the light coming from the stellar disk, inducing a $\sim 1\%$ decrease in the star's observed intensity. By combining the photometric measurement of the transit light curve with a spectroscopic measurement of the planet's orbit, both the planet radius r_p and mass m_p can be derived. Such an intrinsic planetary characterization can only be done for transiting planets. By comparing the measured r_p and m_p with planetary models (e.g., Guillot et al. 2005, Fortney et al. 2007) the planet's structure and composition can be inferred. This, in turn, can be used to test predictions of planetary formation and evolution theories (Pollack et al. 1996, Boss 1997). In addition, transiting planets allow the study of their atmospheres (Charbonneau et al. 2007 and references therein), the measurement of the alignment, or lack of it, between the stellar spin and planetary orbital angular momentum (e.g., Winn et al. 2005) and the search for a second planet in the system (Agol et al. 2005, Holman & Murray 2005). For the reasons detailed above it is clear that transiting planets are an important tool for extending our understanding of the planet phenomenon, hence the importance of searching for them.

The combination of the light collecting area, large FOV (0.31 deg^2) and short read-out time, makes the C18 a useful tool for obtaining high-quality transit light curves for relatively bright stars. The large FOV is especially important, since it allows one to observe many comparison stars, similar in brightness and color to the target, which is crucial for the accurate calibration of the target's brightness. Currently the C18 is used for obtaining transit light curves for several projects, two of which are:

- *Photometric follow-up of transiting planet candidates*: Over the last few years small-aperture wide-field ground-based telescopes have been used to detect ~ 15 transiting planets⁸. This is about half of all known such planets and the discovery rate of these instruments is increasing. Once a transit-like light curve is identified by these small telescopes it is listed as a transiting planet *candidate*, to be followed-up photometrically and spectroscopically, discriminating between true planets and false positives (e.g., O'Donovan et al. 2007), and measuring the system's parameters. Photometric follow-up observations to obtain a high-quality transit light curve are carried out to verify the detection and measure several system parameters, including the planet radius and mid-transit time. Spectroscopic follow-up is used for measuring the companion's orbit from which its mass is inferred.

⁸For an updated list of known transiting planets see: <http://obswww.unige.ch/~pont/TRANSITS.htm>

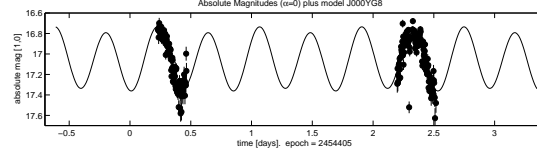


Fig. 8.— Light curve model fit to the observed photometry data for asteroid (106836) 2000 YG₈.

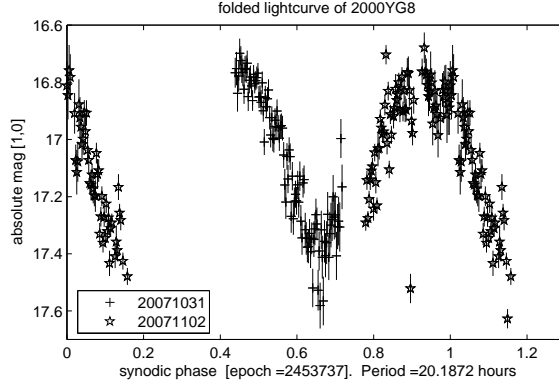


Fig. 9.— Light curve of the asteroid (106836) 2000 YG₈, with the photometric data folded with a period of 20.1872 hours.

The C18 is used for photometric following-up of candidates identified in data obtained by the WHAT telescope (Shporer et al. 2007), in collaboration with the HATNet telescopes (Bakos et al. 2006).

- *Photometric follow-up of planets discovered spectroscopically:* Most of the ~ 270 extrasolar planets known today were discovered spectroscopically, i.e., through the radial velocity (RV) modulation of the star induced by the planet, as the two bodies orbit the joint center of mass. The probability that such a planet will show transits is $\frac{r_s + r_p}{d_{tr}}$, where r_s and r_p are the stellar and planetary radii, respectively, and d_{tr} is the planet-star distance at the predicted transit time. This probability is about 1:10 for planets with close-in orbits, with orbital periods of several days. Interestingly, the first extrasolar planet for which transits were observed, HD209458 (Charbonneau et al. 2000, Henry et al. 2000) was the tenth close-in planet discovered spectroscopically (Mazeh et al. 2000). The C18 is taking part in follow-up observations of planets detected spectroscopically, especially those newly discovered, in order to check whether they show a transit signal. The remote operation makes it possible to carry out observations on very short notice. Observations made with the C18 were part of the discovery of the transiting nature of Gl 436 b (Gillon et al. 2007), a Neptune-mass planet orbiting an M dwarf (Butler et al. 2004, Maness et al. 2007).

During an observation of a transit, the PSF is monitored and the exposure time is adjusted from time to time, keeping the target count level from changing significantly. A guide star is usually used. After bias, dark and flat-field corrections, images are processed with the IRAF/phot task, using a few trial aperture radii. The target light curve is calibrated using a few dozen low-RMS stars similar in brightness to the target. As a final step, the out-of-transit measurements are fitted to several parameters, such as airmass, HJD and PSF FWHM, and all measurements are divided by the fit.

An example of a transit light curve obtained with the C18 is shown in Figure 11; this is the light curve of a HATNet candidate (Internal ID HTR176-003). The top panel shows the actual light curve and the bottom panel shows the light curve binned in 5 minute bins. The residual RMS of the unbinned measurements is 0.22 %, or 2.4 milli-magnitude, and for the binned light curve it is 0.09 %, or 1.0 milli-magnitude. Figure 12 presents the RMS vs. mean V magnitude for all the stars identified in this field. The X-axis is in instrumental magnitude, which is close to the real magnitude. The RMS of the brightest stars reaches below the 3 milli-magnitude level (see also Winn *et al.* 2007).

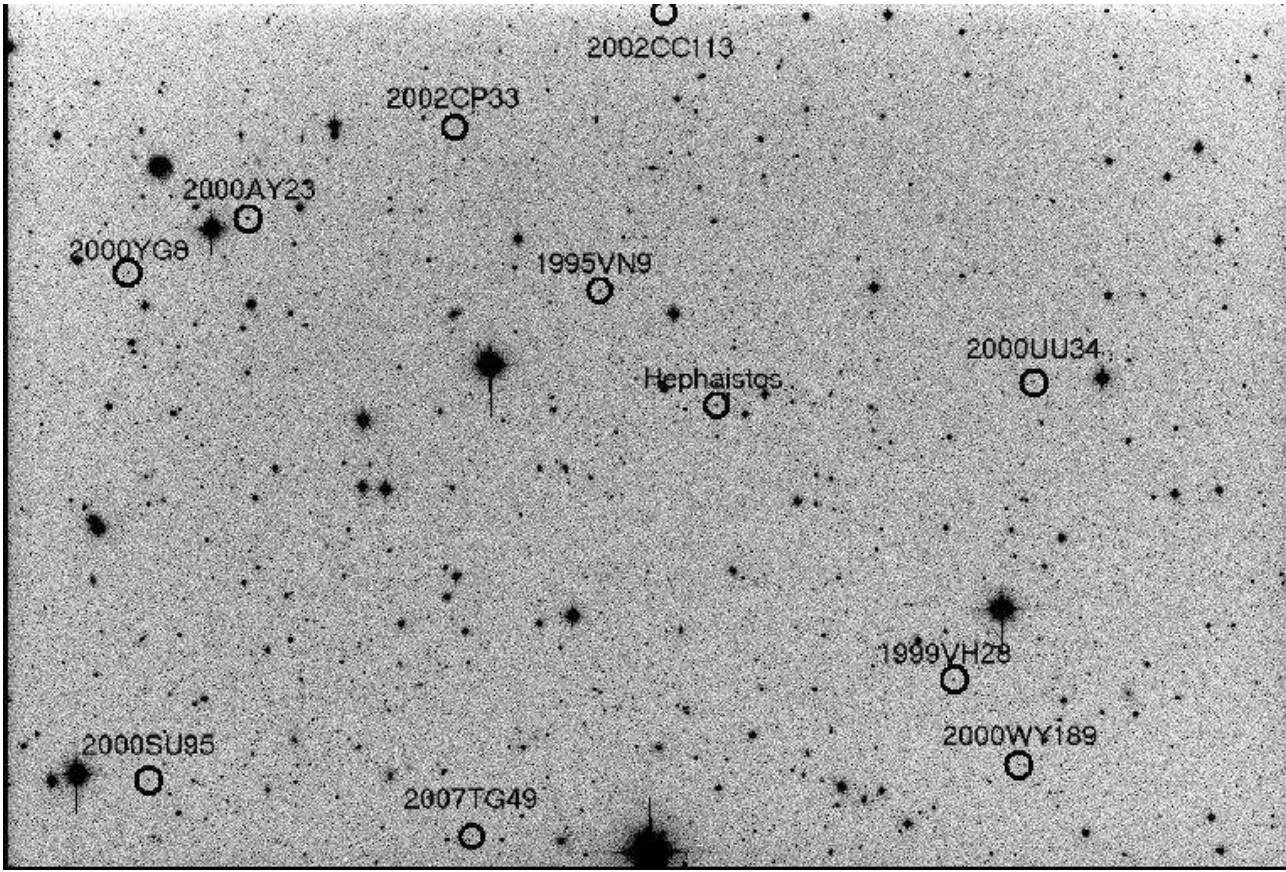


Fig. 10.— Eleven asteroids appear on this wide field ($40.5' \times 27.3'$) image obtained with the C18 (displayed here as negative). Each asteroid is labelled with its name and is marked by a circle. The field was followed for 7.75 hours and the light curve of each asteroid was measured. The asteroid (106836) 2000 YG₈ appears in the upper-left corner.

9.3 AGN monitoring

The C18 fits the requirements for monitoring Active Galactic Nuclei (AGNs). Such objects are known for their continuum variability and, though the origin of this variability is still unclear, it is possible to use it to study, using various techniques, the physical conditions in the AGNs and their properties. One such technique, which enables the study of the emission-line gas and the measuring of the central supermassive black hole mass in AGNs, is the “reverberation mapping” (e.g., Peterson et al. 1993). In such studies, the time lag between the variations in the continuum flux and the emission-line fluxes is used to estimate the Broad Line Region (BLR) size, and to map its geometry.

Combining such time lags with the BLR velocity (measured from the width of the emission-lines) allows the determination of the black hole mass in an AGN (e.g., Kaspi et al. 2000, Peterson et al. 2004). The WO took a leading role in such studies, carrying out about half of all reverberation mapping studies ever done.

An important empirical size-mass-luminosity relation, spanning a broad luminosity range, has been derived for

AGNs based on 36 AGNs with reverberation mapping data. This is now widely used to determine the black hole mass from single-epoch spectra for large samples of AGNs and distant quasars, allowing the study of black hole growth and its effect on galaxy evolution. However, more reverberation mapping studies are needed to expand the luminosity range and to re-define the current relation with better statistics (i.e., adding more objects to the 36 already studied).

One crucial element in reverberation mapping studies is the continuous monitoring of the continuum flux variations. For low-luminosity AGNs, which vary on timescales of hours to days, it is important that the monitoring period of several days will be densely covered at a sampling rate of several minutes. To achieve such coverage the close collaboration of several observatories around the world is essential.

One such study, carried out with the C18, is the monitoring of the low-mass candidate AGN SDSS J143450.62+033842.5 (Greene & Ho 2004; $z = 0.0286$, $m_r = 15$). During a one-week period in April 2007 this AGN was monitored with a typical exposure time of 240 sec. The images were reduced in the same way as described in Section 9.1. The typical uncertainty of the measurements

is about 0.1 magnitude which is sufficient to detect the variability of this AGN. Figure 13 shows the light curve, derived using differential photometry and the “daostat” program described in Netzer et al. (1996, section 2.3).

Combining this light curve with additional data from the Crimean Astrophysical Observatory in Ukraine, the MAGNUM-2m telescope in Hawaii, and the 2m Faulkes Telescope in Australia, produced a fully-sampled continuum light curve for SDSS J143450.62+033842.5 covering several days. Together with an emission-line light curve obtained at the Magellan telescope, the central mass of the black hole in the center of this AGN will be determined. The C18 based at the WO played a crucial part in this monitoring campaign and proved that it can be most useful in producing AGN light curves, which are used in state-of-the-art studies of supermassive black holes.

10 Conclusions

We described the construction of a secondary observing facility at the Wise Observatory, consisting of a 0.46m Prime Focus f/2.8 telescope equipped with a good quality commercial CCD camera. The C18 telescope and camera are sited in a small fiberglass dome, with a suite of programs using ASCOM interface capability orchestrating the automatic operation. The combination offers a cost-effective way of achieving a limited goal: the derivation of high-quality time-domain sampling of various astronomical sources.

The automatic operation, despite the few snags discovered following two years of operation, proves to be very user-friendly since it allows the collection of many observations without requiring the presence of the observer at the telescope or even at the Wise Observatory. This was achieved with a very modest financial investment and may be an example for other astronomical observatories to follow.

We presented results from three front-line scientific projects performed with the new facility, which emphasize the value of an automated and efficient, relatively wide-field, small telescope.

Acknowledgments

The C18 telescope and most of its equipment were acquired with a grant from the Israel Space Agency (ISA) to operate a Near-Earth Asteroid Knowledge Center at Tel Aviv University. DP acknowledges an Ilan Ramon doctoral scholarship from ISA to study asteroids. We are grateful to the Wise Observatory Technical Manager Mr. Ezra Mash’al, and the Site Manager Mr. Sammy Ben-Guigui, for their dedicated contribution in erecting the C18 facility and repairing the many small faults discovered during the first two years of operation.

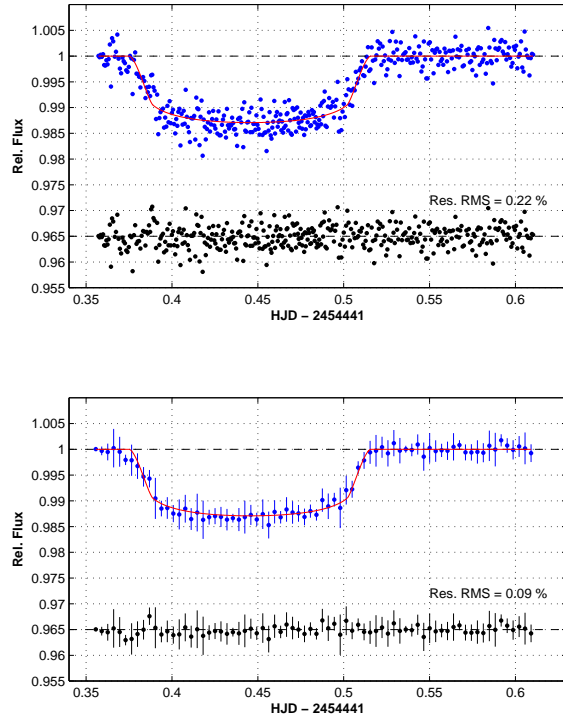


Fig. 11.— Light curve of a HATNet transiting planet candidate obtained by the C18. Both panels show relative flux vs. time. The top panel presents the actual measurements (blue points) overplotted by a fitted model (solid red line). Residuals from the fitted model are also plotted (black points), shifted to a zero point of 0.965. In the bottom panel, blue points and error bars represent a 5 min mean and RMS. The same model is overplotted (solid red line) and residuals (in black) are also shifted to a zero point of 0.965. Each of the 5 min bins includes 5.3 measurements on average. The RMS of the residuals of the actual measurements is 0.22 %, or 2.4 milli-magnitude, and for the binned light curve, 0.09 %, or 1.0 milli-magnitude. This light curve includes 400 individual measurements taken during 6.2 hours, with an exposure time of ~ 25 sec for each frame.

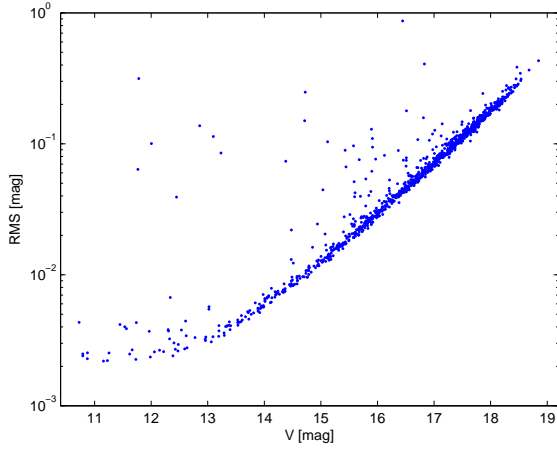


Fig. 12.— RMS vs. mean V magnitude for all stars identified in the field of the transiting planet candidate shown in Fig. 11. Y-axis is in log scale and X-axis is in instrumental magnitude, although this is close to the real magnitude. Observations were done on a single night with a typical exposure time of 25 seconds. For the brightest stars, the RMS reaches below the 3 milli-magnitude level.

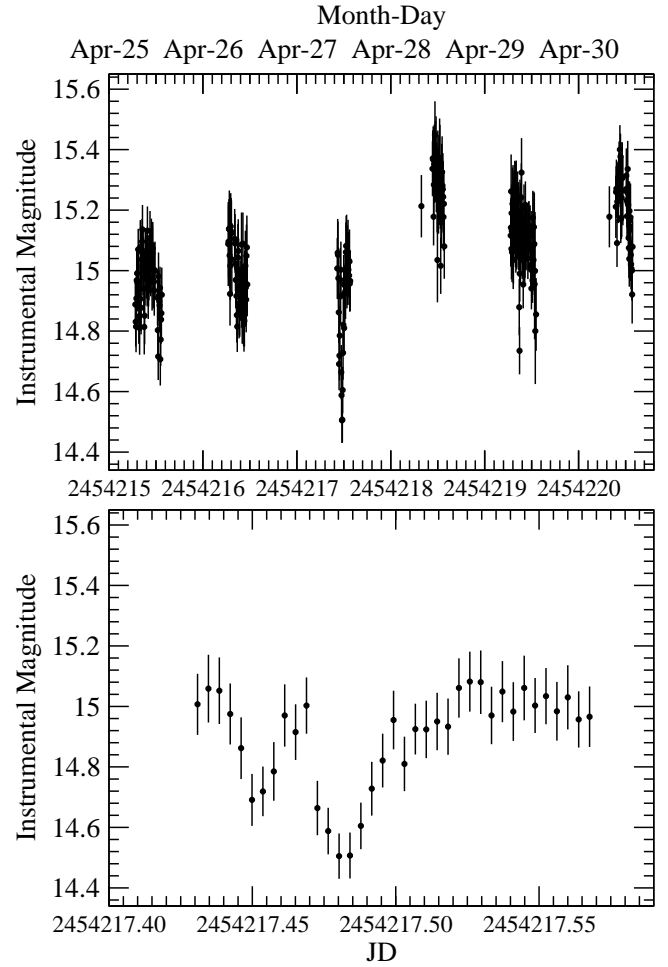


Fig. 13.— Light curve of the low-luminosity AGN SDSS J143450.62+033842.5. The full-resolution light curve of the entire monitoring run is shown in the top panel and a zoomed-in view of the third monitoring night is shown in the bottom panel. Flux variations on timescales of hours to days are clearly detected.

References

- Agol, E., Steffen, J., Sari, R., & Clarkson, W. 2005, MNRAS, 359, 567
- Akerlof, C. W., et al. 2003, PASP, 115, 132
- Bakos, G., Noyes, R. W., Kovács, G., Stanek, K. Z., Sasselov, D. D., & Domsa, I. 2004, PASP, 116, 266
- Bakos, G., Noyes, R. W., Latham, D. W., Csák, B., Gálfi, G., & Pál, A. 2006, Tenth Anniversary of 51 Peg-b: Status of and prospects for hot Jupiter studies, 184
- Barthelmy, S.D. et al. 1998, in *Gamma-Ray Bursts: 4th Huntsville Symposium*, C.A. Meegan, R.D. Preece, T.M. Koshut (eds.), AIP Conf. Proc. **428**, 99
- Boss, A. P. 1997, Science, 276, 1836
- Bowell, E., Hapke, B., Domingue, D., Lumme, K., Peltoniemi, J. and Harris, A. W., 1989. *Application of photometric models to asteroids*. In Asteroids II (R. P. Binzel, T. Gehrels and M. S. Matthews, Eds.), pp. 524-556. Univ. of Arizona Press, Tucson
- Bowen, I. and Vaughan, A. H., Jr., 1973, Applied Optics **12**, 1430.
- Brosch, N. 1992, Q.J.R.astr.Soc. **33**, 27
- Butler, R. P., Vogt, S. S., Marcy, G. W., Fischer, D. A., Wright, J. T., Henry, G. W., Laughlin, G., & Lissauer, J. J. 2004, ApJ, 617, 580
- Charbonneau, D., Brown, T. M., Latham, D. W., & Mayor, M. 2000, ApJ, 529, L45
- Charbonneau, D., Winn, J. N., Everett, M. E., Latham, D. W., Holman, M. J., Esquerdo, G. A., & O'Donovan, F. T. 2007, ApJ, 658, 1322
- Gillon, M., et al. 2007, A&A, 472, L13
- Greene, J. E., & Ho, L. C. 2004, ApJ, 610, 722
- Guillot, T. 2005, Annual Review of Earth and Planetary Sciences, 33, 493
- Fortney, J. J., Marley, M. S., & Barnes, J. W. 2007, ApJ, 659, 1661
- Harris, A. W. and Lupishko, D. F., 1989. *Photometric light curve observations and reduction techniques*. In Asteroids II (R. P. Binzel, T. Gehrels and M. S. Matthews, Eds.), pp. 39-53. Univ. of Arizona Press, Tucson.
- Henry, G. W., Marcy, G. W., Butler, R. P., & Vogt, S. S. 2000, ApJ, 529, L41
- Holman, M. J., & Murray, N. W. 2005, Science, 307, 1288
- Kaspi, S., Smith, P. S., Netzer, H., Maoz, D., Jannuzi, B. T., & Givon, U. 2000, ApJ, 533, 631
- Landolt, A., 1992. AJ **104**, no. 1, 340
- Maness, H. L., Marcy, G. W., Ford, E. B., Hauschildt, P. H., Shreve, A. T., Basri, G. B., Butler, R. P., & Vogt, S. S. 2007, PASP, 119, 90
- Mazeh, T., et al. 2000, ApJ, 532, L55
- Netzer, H., et al. 1996, MNRAS, 279, 429
- O'Donovan, F. T., et al. 2007, ApJ, 662, 658
- Pepper, J., et al. 2007, PASP, 119, 923
- Peterson, B. M. 1993, PASP, 105, 247
- Peterson, B. M., et al. 2004, ApJ, 613, 682
- Polishook, D. & Brosch N., Icarus, in press (astro-ph/0607128)
- Pollacco D. L., et al., 2006, PASP, 118, 1407.
- Pollack, J. B., Hubickyj, O., Bodenheimer, P., Lissauer, J. J., Podolak, M., & Greenzweig, Y. 1996, Icarus, 124, 62
- Shporer, A., Mazeh, T., Moran, A., Bakos, G., & Kovacs, G. 2007, Transiting Extrapolar Planets Workshop, 366, 99
- Steele I. A., et al., 2004, SPIE, 5489, 679.
- Yost S. A., et al., 2006, AN, 327, 803.
- Zerbi R. M., et al., 2001, AN, 322, 275.
- Winn, J. N., et al. 2005, ApJ, 631, 1215
- Winn, J. N., Holman, M. J., & Roussanova, A. 2007, ApJ, 657, 1098